

## Initial Steps of the Sol–Gel Process: Modeling Silicate Condensation in Basic Medium

Henning Henschel,<sup>†,§</sup> Andreas M. Schneider,<sup>‡</sup> and Marc H. Prosen<sup>\*,†</sup>

<sup>†</sup>Department für Chemie, Institut für Anorganische und Angewandte Chemie, Universität Hamburg, Martin-Luther-King Platz 6, D-20146 Hamburg, Germany, and <sup>‡</sup>Institut für Anorganische Chemie, and Zentrum für Festkörperchemie und Neue Materialien, Leibniz Universität Hannover, Callinstr. 9, D-30167 Hannover, Germany. <sup>§</sup>Present address: Bioorganic & Biophysical Chemistry Laboratory, School of Natural Sciences, Linnæus University, SE-391 82 Kalmar, Sweden.

Received February 8, 2010. Revised Manuscript Received July 1, 2010

The initial step of the sol–gel process, that is, the condensation of two molecules of silicic acid has been studied by means of density functional theory. The chosen system represents the reagents under basic reaction conditions. Calculations were performed in the gas phase as well as by employing a solvent model for aqueous solution. For both systems, a reaction intermediate with one pentacoordinated silicon center was found as the most stable structure. The influence of intramolecular hydrogen bonds on the stability of the intermediate structure is discussed, and different pathways for the subsequent condensation step are investigated. Furthermore, the effect of fluoride substitution on the reaction path is investigated.

### Introduction

The sol–gel process is a widely used method to synthesize a broad selection of materials. Its main application is on silicate materials, which can be synthesized with great homogeneity and purity under relatively mild conditions.<sup>1</sup> It is also of particular importance for the synthesis of zeolites.<sup>2</sup> In order to achieve a better understanding of structure formation in zeolites and related materials and thus be able to better influence the properties of materials, it is of great importance to get insight into the mechanism underlying the sol–gel process. Even though a large

number of theoretical studies<sup>3–20</sup> of related systems and experimental<sup>21–32</sup> studies on the mechanisms of silicate condensation have been published, still there is no consistent picture of the reaction path and mechanism of either the base-catalyzed or the acid-catalyzed sol–gel process to be found in the literature.<sup>19,33</sup> The most commonly encountered picture is that of an S<sub>N</sub>2 like mechanism with a pentacoordinated silicon atom only in the transition state,<sup>3,4,6,10,16–20</sup> while others predict for certain reaction conditions an (compared to substrate and/or product complex) energetically unfavorable intermediate structure containing a pentacoordinated silicon atom.<sup>12,14,15,19</sup>

\*To whom correspondence should be addressed. E-mail: prosenc@chemie.uni-hamburg.de.

- (1) Henschel, L. L.; West, J. K. *Chem. Rev.* **1990**, *90*, 33–72.
- (2) Cheetham, A. K.; Mellot, C. F. *Chem. Mater.* **1997**, *9*, 2269–2279.
- (3) Ignatyev, I. S.; Partal, F.; González, J. L. *Chem. Phys. Lett.* **2003**, *368*, 616–624.
- (4) Ignatyev, I. S.; Montejo, M.; González, J. L. *ChemPhysChem* **2009**, *10*, 940–945.
- (5) Kubicki, J. D.; Xiao, Y.; Lasaga, A. C. *Geochim. Cosmochim. Acta* **1993**, *57*, 3847–3853.
- (6) Okumoto, S.; Fujita, N.; Yamabe, S. *J. Phys. Chem. A* **1998**, *102*, 3991–3998.
- (7) Gordon, M. S.; Carroll, M. T.; Davis, L. P.; Burggraf, L. W. *Comput. Mater. Sci.* **1993**, *1*, 161–168.
- (8) Elanany, M.; Selvam, P.; Yokosuka, T.; Takami, S.; Kubo, M.; Imamura, A.; Miyamoto, A. *J. Phys. Chem. B* **2003**, *107*, 1518–1524.
- (9) Ermoshin, V. A.; Smirnov, K. S.; Bougeard, D. *J. Mol. Struct. (Theochem)* **1997**, *393*, 171–176.
- (10) Pereira, J. C. G.; Catlow, C. R. A.; Price, G. D. *Chem. Commun.* **1998**, *13*, 1387–1388.
- (11) Lasaga, A. C.; Gibbs, G. V. *Am. J. Sci.* **1990**, *290*, 263–295.
- (12) Xiao, Y.; Lasaga, A. C. *Geochim. Cosmochim. Acta* **1996**, *60*, 2283–2295.
- (13) Mora-Fonz, M. J.; Catlow, C. R. A.; Lewis, D. W. *J. Phys. Chem. C* **2007**, *111*, 18155–18158.
- (14) Trinh, T. T.; Jansen, A. P. J.; van Santen, R. A. *J. Phys. Chem. B* **2006**, *110*, 23099–23106.
- (15) Trinh, T. T.; Jansen, A. P. J.; van Santen, R. A.; Meijer, E. J. *J. Phys. Chem. C* **2009**, *113*, 2647–2652.

- (16) Pelmenchikov, A.; Strandh, H.; Petterson, L. G. M.; Leszczynski, J. *J. Phys. Chem. B* **2000**, *104*, 5779–5783.
- (17) Feuston, B. P.; Garofalini, S. H. *J. Phys. Chem.* **1990**, *94*, 5351–5356.
- (18) Martin, G. E.; Garofalini, S. H. *J. Non-Cryst. Solids* **1994**, *171*, 68–79.
- (19) Schaffer, C. L.; Thomson, K. T. *J. Phys. Chem. C* **2008**, *112*, 12653–12662.
- (20) Kudo, T.; Gordon, M. S. *J. Am. Chem. Soc.* **1998**, *120*, 11432–11438.
- (21) Kinrade, S. D.; Swaddle, T. W. *Inorg. Chem.* **1988**, *27*, 4259–4264.
- (22) Kinrade, S. D.; Swaddle, T. W. *Inorg. Chem.* **1988**, *27*, 4253–4259.
- (23) Kinrade, S. D.; Knight, C. T. G.; Pole, D. L.; Syvitski, R. T. *Inorg. Chem.* **1998**, *37*, 4278–4283.
- (24) Kinrade, S. D.; Pole, D. L. *Inorg. Chem.* **1992**, *31*, 4558–4563.
- (25) Klemperer, W. G.; Ramamurthi, S. D. *Mater. Res. Soc. Symp. Proc.* **1988**, *121*, 3–13.
- (26) Murthy, V. S.; Miller, J. M. *Inorg. Chem.* **1995**, *34*, 4513–4515.
- (27) Pouxviel, J. C.; Boilot, J. P. *J. Non-Cryst. Solids* **1987**, *94*, 374–386.
- (28) Pouxviel, J. C.; Boilot, J. P.; Beloeil, J. C.; Lallemand, J. Y. *J. Non-Cryst. Solids* **1987**, *89*, 345–360.
- (29) Zerda, T. W.; Hoang, G. *Chem. Mater.* **1990**, *2*, 372–376.
- (30) Pelster, S. A.; Kalamajka, R.; Schrader, W.; Schüth, F. *Angew. Chem., Int. Ed.* **2007**, *119*, 2349–2352.
- (31) Pelster, S. A.; Bruno Weimann; Schaack, B. B.; Schrader, W.; Schüth, F. *Angew. Chem., Int. Ed.* **2007**, *119*, 6794–6797.
- (32) Bussian, P.; Sobott, F.; Brutschy, B.; Schrader, W.; Schüth, F. *Angew. Chem., Int. Ed.* **2000**, *112*, 4065–4069.
- (33) Pinkas, J. *Ceram-Silikaty* **2005**, *49*, 287–298.

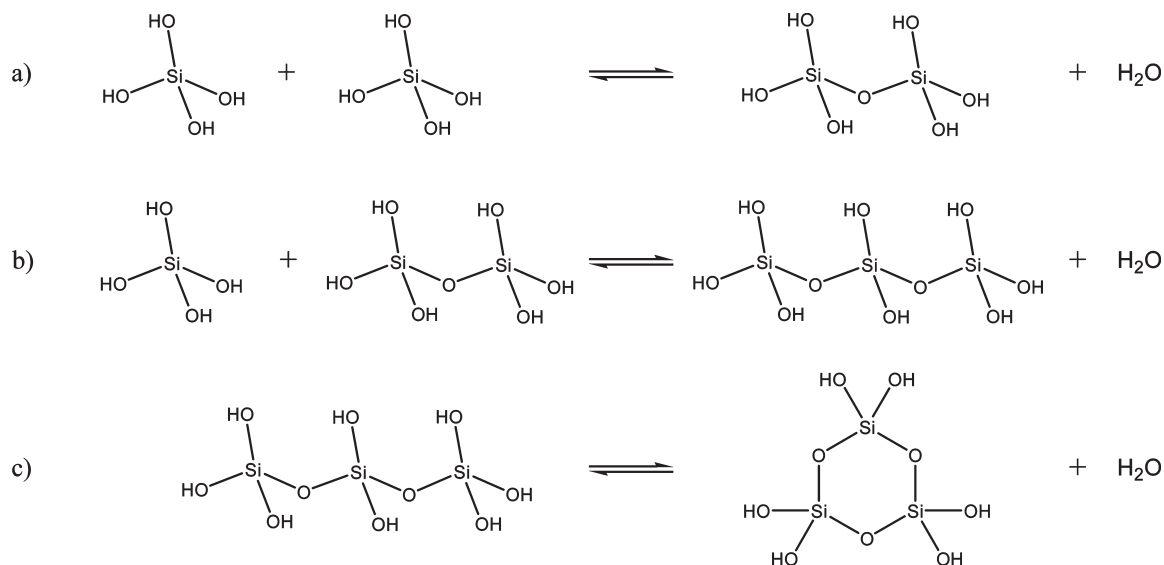


**Figure 1.** Silica condensation reaction: (a) dimerization; (b) trimerization; and (c) cyclization.

Orthosilicic acid with a  $\text{p}K_a$  of 9.9 is a very weak acid; protonation in strong acid medium below pH 2, the isoelectric point, where orthosilicic acid appears as a neutral molecule, is possible. Orthosilicic acid stays stable in water at 298 K for a long period up to a concentration of 2 mM ( $\sim 40$  ppm). Above this concentration, rapid condensation takes place. The solubility of orthosilicic acid is higher than 2 mM due to the formation of still soluble oligomeric compounds. However, the solubility of amorphous silica is strongly dependent on the pH. It ranges from 100 to 150 ppm (pH 0–8) with a possible minimum around pH 7–8 and increases moderately toward lower pH values. Toward higher pH, the solubility shows strong ascent up to 1000 ppm in the basic regime.<sup>34</sup> The reaction takes place either above or below the isoelectric point of silicic acid (pH 2) involving a deprotonated anionic monomer or a protonated cationic monomer, respectively. Since the amount of the ionic species is rather low due to the  $\text{p}K_a$  of 9.9, the condensation reaction does not take place at the isoelectric point; the concentration of the ionic species is rate-determining for the condensation reaction. During condensation steps taking place after the dimerization, the species with higher degree of condensation is the charged one since its  $\text{p}K_a$  value is lower.

Starting with the trimer, ring closure reactions are possible and preferred due to the larger number of individual molecules formed. The most stable species in the following reaction cascade are most probably the cyclic tetramer, the hexagonal prism, and the cubic octamer, which is assumed to be the predominant starting point of particle growth.<sup>1,34–37</sup>

In this work, we present theoretical investigations into the first step of silica oligomerization ((route a) depicted

in Figure 1) with the main emphasis on possible intermediate structures along the condensation path.

### Theoretical Basis

For DFT calculations performed, a B3LYP functional according to Becke<sup>38</sup> has been used. For all calculations, the program package Gaussian 03<sup>39</sup> has been employed with a 6-31G\* basis set<sup>40</sup> as supplied with the program. Geometries have been optimized using a cutoff of  $10^{-8}$  for SCF and  $10^{-7}$  for gradients.

Solvation effects were included in the calculations by utilizing a conductor-like screening model (COSMO).<sup>41</sup> The COSMO approach was employed using the dielectricity constant of water ( $\epsilon_{\text{H}_2\text{O}} = 78.39$ ).

Association energies of complexes have been calculated as the difference between the calculated energy of the complex and the isolated molecules. All stationary geometries have been checked by frequency calculation, yielding only positive eigenvalues for minima and exactly one negative eigenvalue for transition states. Transition states were confirmed to correspond to the desired transformation by calculation of the intrinsic reaction coordinate (IRC).

### Results

To probe alternative reaction pathways for silicate condensation, a simple model system, based on the studies conducted by Sjöberg et al.,<sup>42,43</sup> was chosen. The system represents the condensation reaction of a singly deprotonated silicic acid ion ( $\text{Si(OH)}_3\text{O}^-$ ) and a silicic acid molecule ( $\text{Si(OH)}_4$ ).

(34) Iler, R. K. *The Chemistry of Silica*; Wiley-Interscience: New York, 1979.

(35) Pelster, S. A.; Weimann, B.; Schaack, B. B.; Schrader, W.; Schüth, F. *Angew. Chem., Int. Ed.* **2007**, *46*, 6674–6677.

(36) Schaack, B. B.; Schrader, W.; Schüth, F. *Angew. Chem., Int. Ed.* **2008**, *47*, 9092–9095.

(37) Garofalini, S. H.; Martin, G. J. *J. Phys. Chem.* **1994**, *98*, 1311–1316.

(38) Becke, A. D. *J. Chem. Phys.* **1993**, *98*, 5648–5652.

(39) Frisch, M. J. et al. Gaussian 03, revision B.01, Gaussian, Inc.: Wallingford, CT, 2004.

(40) Hehre, W. J.; Ditchfield, R.; Pople, J. A. *J. Chem. Phys.* **1972**, *56*, 2257–2261.

(41) Barone, V.; Cossi, M. *J. Phys. Chem. A* **1998**, *102*, 1995–2001.

(42) Sjöberg, S.; Öhman, L.-O.; Ingri, N. *Acta Chem. Scand. A* **1985**, *39*, 93–107.

(43) Leung, K.; Nielsen, M. B.; Criscenti, L. J. *J. Am. Chem. Soc.* **2009**, *131*, 18358–18365.

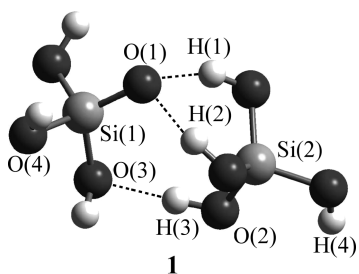


Figure 2. Optimized structure of the substrate complex.

Table 1. Geometrical Parameters of Optimized Substrate Complex 1

$d$ [pm]	<i>in vacuo</i>	COSMO
Si(1)–O(1)	158	159
Si(1)–O	168; 169; 170	168; 168; 170
Si(2)–O(1)	312	310
Si(2)–O	165; 165 166; 167	165; 166 166; 166
O(1)–H(1)	179	175
O(1)–H(2)	178	174
H(3)–O(3)	190	184

Optimization of the initial state of the condensation reaction yielded a complex in which the silicic acid and the silicic acid anion are connected by three hydrogen bonds with bond lengths  $d(\text{O}(1)\text{--H}(1)) = 179$  pm,  $d(\text{O}(1)\text{--H}(2)) = 178$  pm, and  $d(\text{O}(3)\text{--H}(3)) = 190$  pm (**1**, Figure 2). Geometrical parameters of structure **1** are listed in Table 1. In the initial complex **1**, the Si–Si distance is calculated to be only 388 pm, which is indicative of a strongly bound hydrogen bridged dinuclear silicic acid complex. The dissociation energy of the two moieties is calculated to be 188.0 kJ/mol in the gas phase. When a COSMO solvent model is applied, the geometrical parameters do not change significantly (Table 1); however, the calculated dissociation energy is reduced to 100.3 kJ/mol. In addition to the intermolecular hydrogen bond, interactions between O(1) and two adjacent hydroxyl hydrogen atoms, interactions between O(3)–H and O(4) and between H(4) and O(2) are found. All of this leads to the strong association of the orthosilicic acid molecule with the monoanion of orthosilicic acid.

To model the condensation reaction, a preliminary reaction profile for the formation of the Si–O bond was calculated by reducing the Si(2)–O(1) distance by 10 pm within 20 steps while optimizing all other coordinates.

Starting from **1**, reaction intermediate **2** was reached by reducing the O(1)–Si(2) distance. Along the reaction path, at a Si–O distance of 244 pm a transition state (**TS1**, structure presented in Supporting Information) with an energy of 24.2 kJ/mol (28.0 kJ/mol COSMO) above structure **1** has been located. Further reduction of the Si(2)–O(1) distance to 186 pm revealed the intermediate complex **2**.

The energy profile of the formation reaction of **2** from **1** is depicted in Figure 3. This reaction path leading through the energetically most favorable transition state does not connect the lowest energy structures of **1** and **2** directly. However, the structures it leads to (denoted **1**<sup>#</sup> and **2**<sup>#</sup>, respectively) are separated from the lowest energy structures only by reorientation of the hydroxyl groups.

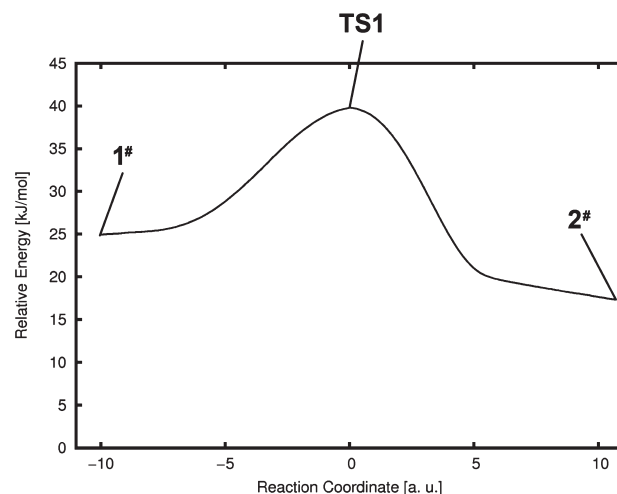


Figure 3. Reaction coordinate of the formation reaction of **2** from **1**. Please note that the end structures of the coordinate are not the lowest energy conformers of the respective structure.

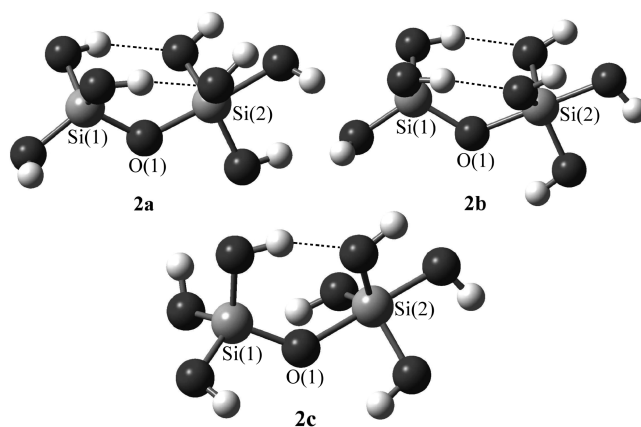


Figure 4. *In vacuo* optimized structures of the intermediate complexes. Structures optimized using COSMO are essentially identical (see Table 2).

Table 2. Geometrical Parameters of Optimized Intermediate Structures 2

$d$ [pm]	<i>In Vacuo</i>			COSMO			
	2a	2b	2c	2'a	2'b	2'c	2'd
Si(1)–O(1)	163	163	161	162	163	162	162
Si(1)–O	166	166	166	166	166	166	166
	167	167	167	166	166	166	166
	167	167	168	166	166	167	167
Si(2)–O(1)	173	177	186	177	179	183	188
Si(2)–O <sub>eq</sub>	170	171	170	170	170	170	170
	172	172	171	172	172	171	170
	174	173	173	173	172	173	174
Si(2)–O <sub>ax</sub>	184	179	174	178	176	175	173
OH–O <sub>br</sub> <sup>a</sup>	190	190	177	185	184	175	195
	190	191		186	185		

<sup>a</sup> Hydrogen bond bridging oxygen atoms adjacent to the two different silicon centers.

For intermediate **2**, three stable conformers were located (see Figure 4). The structures exhibit an oxygen atom O(1) bridging the two silicon centers, one of which (Si(1)) is tetracoordinated with a distorted tetrahedral geometry and the other one (Si(2)) pentacoordinated with a distorted trigonal-bipyramidal coordination geometry. For **2**, four different orientations of intramolecular hydrogen



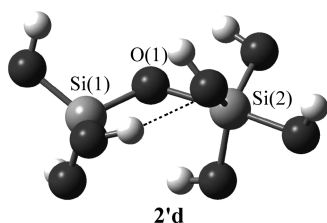


**Figure 5.** COSMO-optimized structure of the *in vacuo*-unstable intermediate.

bonds are feasible. Of the three OH-groups equatorially bound to the pentacoordinated silicon atom Si(2), none (**2a**), one (**2b**), two (**2c**), or all three (**2d**) can point with their hydrogen atom toward one of the oxygen atoms bound to Si(1). Structure **2d** is labile (therefore not depicted); it optimizes into starting complex **1**. Optimization of structures **2a**, **2b**, and **2c** *in vacuo*, however, yielded an energy minimum (Figure 4) with structure **2b** calculated to be the most stable. The energy for structure **2b** *in vacuo* is calculated to be  $-20.8$  kJ/mol relative to that of initial state **1** and  $-30.4$  and  $-24.5$  kJ/mol relative to the energies of **2a** and **2c**, respectively. The short O(1)–Si(2) distance of 177 pm found for **2b** is comparable to those reported in the literature for experimental<sup>44</sup> and theoretical studies<sup>5,6,10,45</sup> of pentaoxocoordinated silicon compounds. Although structure **2a** is calculated to be a minimum on the energy surface, its energy of formation from **1** is positive, i.e., the structure is not stable.

The unexpected stability of **2b** and **2c** in contrast to **2a** and **2d** requires further clarification. It can be clearly seen that the energy of structure **2** is highly dependent on the geometry of the hydrogen bonds. The lack of stability of **2d** toward dissociation to **1** (see Figure 5 for the corresponding COSMO-optimized structure) can be ascribed to the fact that only in this structure does the oxygen atom of the apical OH-group on Si(2) not interact with a hydrogen atom. Therefore, the negative charge density on this oxygen atom is not compensated. In structure **2a**, the OH $\cdots$ HO interaction of the apical and equatorial hydroxyl groups appears to be the cause of the destabilization. Thus, it can be summarized that the stability of the pentacoordinated configuration of Si(2) in structure **2** relies on a balanced system of O–H interactions. In both cases, with all equatorially bound hydroxido ligands directed the same way, the system was found to be unstable. A detailed description of the binding properties of pentacoordinated silicon systems is found in ref 46.

Calculations including solvent influences (water) by means of the COSMO model showed a lower level of dependence of the energy on the conformation of the hydrogen bonds. It was possible to obtain optimized structures of all four conformations (**2'a–d**; for **2'd**, see Figure 5). Similar to the gas phase calculations, in solution, **2'b** was found to be most stable with an energy

of  $-10.9$  kJ/mol relative to that of the corresponding starting complex **1'**. The energy for **2'c** is calculated to be only 3.5 kJ/mol higher than that of **2'b**, and **2'd** was calculated to have an energy of 21.9 kJ/mol relative to it. The relative energy of **2'a** in contrast accounts for 29.7 kJ/mol, which is similar to the situation *in vacuo*. The relatively high energy of **2'a** can be explained by the crowding of hydrogen atoms on the terminal side of the pentacoordinated silicon center. This entails a high concentration of positive charge, which, on the cost of energy, has to be compensated by the polarizable continuum, while the intramolecular repulsion does not get fully balanced. Geometrical parameters of all optimized reaction intermediates are summarized in Table 2.

As discussed above, the calculated energy of **2a–d** depends on the orientation of intramolecular hydrogen bonds. The lower dependence of **2'** on the hydrogen bond configuration can be explained by the shielding of charges by the polarizable cavity used as the solvent model. In solvents whose molecules can form hydrogen bonds to the intermediate structure, this relative stabilization of the different conformations of **2** is anticipated to be even larger, as these give rise to an additional stabilization of charges that cannot be described using a continuum model.<sup>15,19,47</sup> Additional stabilization of the negative charge of the silicic acid anion and further reaction products could also arise from the interaction with cations present in the solution.<sup>48,49</sup>

Formation of the product structure, the monoanion of disilicic acid (OH)<sub>3</sub>Si–O–Si(OH)<sub>2</sub>O<sup>−</sup>, is achieved by cleavage of a water molecule from the intermediate complex **2**. This has been modeled by, starting from geometry **2b**, increasing the distance between Si(2) and one of the nonbridging oxygen atoms. This elimination of a hydroxido ligand from the pentacoordinated silicon atom was, while optimizing geometries along the putative reaction path, accompanied by a proton transfer from one hydroxido ligand to the leaving group.

A stable geometry for the product complex, representing a deprotonated disilicate ion bound to one water molecule (**3**, Figure 6), has been reached for a distance  $d(\text{Si}(2)\text{--O}) = 314$  pm (325 pm including solvent model). Other geometrical parameters of **3** are to be found in Table 3.

In the *in vacuo* calculations, the energy of complex **3** was calculated to be 6.9 kJ/mol below that of starting complex **1** and 13.9 kJ/mol above that of the most stable intermediate **2b**. Thus, the reaction from **1** to **3** is energetically favored; however, the lowest energy has been found for the reaction intermediate **2**. Calculations employing the COSMO model yield the same energetic ordering of structures, though the energies calculated for **3'** are  $-8.4$  and  $2.5$  kJ/mol relative to **1'** and **2'b**,

(44) Tacke, R.; Burschka, C.; Richter, I.; Wagner, B.; Willeke, R. *J. Am. Chem. Soc.* **2000**, *122*, 8480–8485.

(45) Sefcik, J.; Goddard, W. A., III *Geochim. Cosmochim. Acta* **2001**, *65*, 4435–4443.

(46) Henschel, H.; Prosenc, M. H., manuscript in preparation.

(47) Henschel, H.; Prosenc, M. H.; Schaper, K.; Schneider, A. M. *Recent Research Poster Contribution*; Deutsche Zeolith Tagung: Kiel, Germany, 2009.

(48) Mora-Fonz, M. J.; Catlow, C. R. A.; Lewis, D. W. *J. Phys. Chem. C* **2007**, *111*, 18155–18158.

(49) Strandh, H.; Pettersson, L. G. M.; Sjöberg, L.; Wahlgren, U. *Geochim. Cosmochim. Acta* **1997**, *61*, 2577–2587.

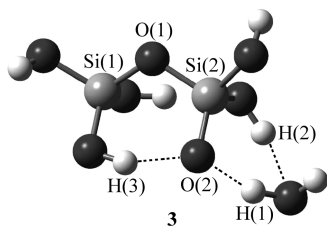


Figure 6. Optimized structure of the product complex.

Table 3. Geometrical Parameters of Optimized Product Complex 3

$d$ [pm]	<i>in vacuo</i>	COSMO
Si(1)–O(1)	165	165
Si(1)–O	165; 166; 166	164; 166; 166
Si(2)–O(1)	168	169
Si(2)–O(2)	158	160
Si(2)–OH	168; 170	167; 168
Si(2)–OH <sub>2</sub>	314	325
H(1)–O(2)	183	162
H(2)–OH <sub>2</sub>	200	187
H(3)–O(2)	170	170

respectively, and thus the reaction in solution is calculated to be slightly more exothermic than in the gas phase.

Alternative reaction pathways for the formation of **3** from **2b** consist of the elimination of different hydroxido ligands from the pentacoordinated silicon center. Two fundamental paths can be distinguished. One of these consists of the abstraction of an equatorially bound hydroxido ligand and the other in the abstraction of the apical hydroxyl group. The abstraction of the apical OH-group from **2b** yields a transition state (TS2, structure presented in Supporting Information) with an energy of 72.6 kJ/mol relative to that of **2b** for the vacuum calculation.

The intrinsic reaction coordinate connecting **2** and **3** is shown in Figure 7. Similar to the reaction path leading through TS1, the reaction coordinate in Figure 7 does not connect the energetically most favorable conformations of **2** and **3** directly.

Abstraction of an equatorially bound group can be regarded as a rather unlikely reaction pathway on the basis of related studies reported by Kubicki et al.<sup>5</sup> and Kudo et al.<sup>20</sup> An alternative to the elimination of equatorially bound water molecule is elimination from a conformation of **2** in which the bridging oxygen atom and by that the tetracoordinated silicon center is bound equatorially to the pentacoordinated silicon atom Si(2) (**2<sub>eq</sub>**, Figure 8, calculated energy 26.5 kJ/mol above **2b**). This geometry can be obtained via a Berry pseudorotation<sup>50</sup> from one of the conformations **2a–c** where the bridging oxygen atom is located in apical position. Structure **2<sub>eq</sub>** has already been suggested as a reaction intermediate by Ermoshin et al.<sup>9</sup> and Xiao and Lasaga.<sup>12</sup> However, we found it to be unstable with respect to **1** and **3**.

The elimination of one water molecule from **2<sub>eq</sub>** to yield product complex **3** proceeds via a transition state whose energy is calculated to be 9.0 kJ/mol higher than that of the transition state between **2b** and **3** (81.6 kJ/mol relative to that of **2b**, 55.1 kJ/mol relative to that of **2<sub>eq</sub>**). The

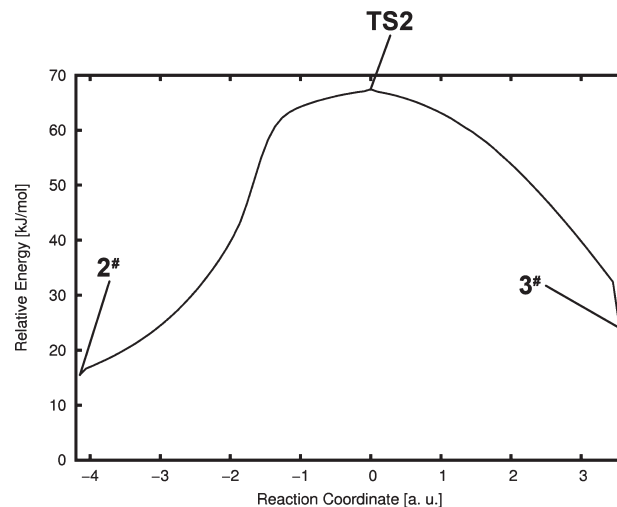


Figure 7. Reaction coordinate of the formation of **3** from **2**. Please note that the ends of the coordinate do not represent the lowest energy conformers of **2** and **3**, respectively.

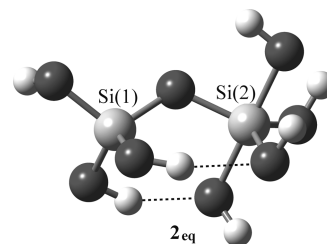


Figure 8. Structure of the intermediate with the bridging oxygen in the apical position.

relative energy for the elimination from **2<sub>eq</sub>** is lower than that for the elimination from **2b**, but as the latter is energetically more favorable, the reaction proceeds by elimination from **2b**. However, this tendency toward a lower activation barrier for the intermediate structures with an equatorially bound silicate unit could be relevant for more highly condensed systems, as in these equatorially linked silicate units become inevitable.

What was discussed above for the stabilization of the different conformations of the intermediate by explicit water molecules is similarly, if not more, relevant for the elimination process. Attached water molecules can facilitate the proton transfer and thus lower the activation barrier.<sup>15,19,20,47</sup> Our study addresses a more general case, i.e., the characteristics of the reaction itself without the influence of one of the numerous molecular level environments occurring during polymerization (e.g., inside a silicate or at sites interacting with template molecules).

The unexpected stability found for the reaction intermediate raises the question as to what influence fluoride ions have on the reaction pathway, as fluoride anions have been reported to stabilize pentacoordinated silicon centers.<sup>51</sup> Furthermore, the presence of fluoride during synthesis of silica materials has been reported to accelerate the formation of zeolite type compounds.<sup>52</sup> In order

(51) Chuit, C.; Corriu, R. J. P.; Reye, C.; Young, J. C. *Chem. Rev.* **1993**, *93*, 1371–1448.

(52) Winter, R.; Chan, J.-B.; Frattini, R.; Jonas, J. J. *Non-Cryst. Solids* **1988**, *105*, 214–222.

(50) Berry, R. S. *J. Chem. Phys.* **1960**, *32*, 933–938.

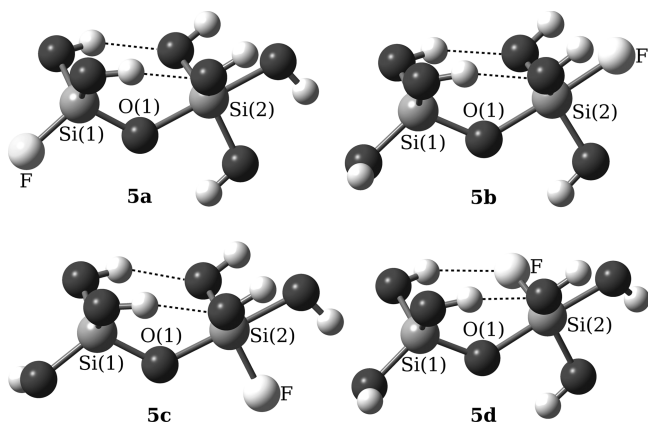


Figure 9. Structures of the examined fluoride substituted intermediates.

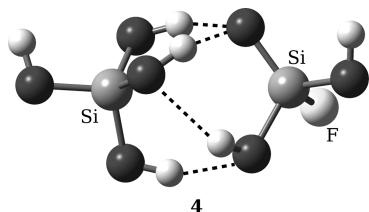


Figure 10. Structure of the fluoride substituted substrate complex.

to study this influence on the condensation reaction, the reaction profile was reinvestigated, substituting one of the hydroxide ions with a fluoride ion as a model system. In the system, four possible isomers were investigated, characterized by the position of the fluorine atom in the reaction intermediate. These structures are illustrated in Figure 9. While in one of the structures the fluoride is bound to the tetracoordinated silicon center (**5a**), in the other structures it occupies the apical (**5b**) and two different equatorial positions (**5c**, **5d**) at the pentacoordinated silicon atom, respectively. All structures were derived from the most stable of the intermediates discussed above (**2b**).

Of the structures depicted in Figure 9, **5b** was found to be most stable, lying energetically 6.4 kJ/mol (24.7 kJ/mol for COSMO) below **5a** and 22.9 kJ/mol (23.6 kJ/mol) and 22.0 kJ/mol (28.0 kJ/mol) below **5c** and **5d**, respectively. By stretching the Si(2)–O(1) bond, a substrate complex is reached, whose most favorable conformation (**4**, Figure 10) lies energetically 26.1 kJ/mol (30.1 kJ/mol) above **2b**. This complex is the same for all intermediate structures, requiring a proton transfer to be involved in the reaction toward **5b**, **5c**, and **5d**. This is in accord with the decreased  $pK_a$  value of F–Si(OH)<sub>3</sub> compared to that of Si(OH)<sub>4</sub>. While in the formation of **5c** and **5d** this proton transfer is simultaneous with the Si–O bond formation, it precedes the nucleophilic attack leading to **5b**, giving a conformation of the substrate complex 14.7 kJ/mol (14.3 kJ/mol) above that of **4** in which the apical position of the fluorine atom is preconfigured.

The transition states of the reactions from the substrate complex **4** to the different intermediates lie at 22.8 kJ/mol (25.5 kJ/mol) for **5a**, 29.0 kJ/mol (28.1 kJ/mol) for **5b**, 67.6 kJ/mol (50.3 kJ/mol) for **5c**, and 66.3 kJ/mol (52.0 kJ/mol) for **5d**, relative to that of **4**.

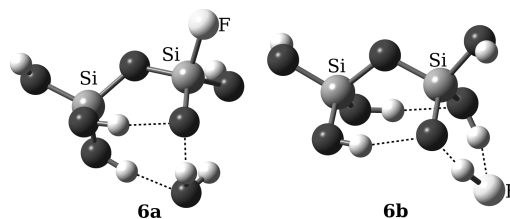


Figure 11. Structure of the fluoride substituted product complexes.

Table 4. Summary of Calculated Energies (Relative to Those of **2b**)

energy [kJ/mol]	1	TS1	2a	2b	2c	2 <sub>eq</sub> /2 <sub>d</sub> <sup>a</sup>	TS2 <sup>b</sup>	3
<i>in vacuo</i>	20.8	45.0	30.4	0	24.5	26.5	72.6 (81.6)	13.9
COSMO	10.9	38.9	29.7	0	3.5	21.9	101.3	2.5

<sup>a</sup> Structure **2<sub>eq</sub>** *in vacuo*; **2<sub>d</sub>** employing COSMO. <sup>b</sup> The value in parentheses is for the transition state between **2<sub>eq</sub>** and **3**.

Table 5. Summary of Calculated Energies of the Fluoride Substituted System (Relative to that of **5b**)

energy [kJ/mol]	isomer	4	TS3	5	TS4	6
<i>in vacuo</i>	a	26.1	49.0	6.4	84.0	6.3
	b		55.1	0	59.9	54.6
	c		93.7	22.9	77.3	6.3
	d		92.4	22.0	105.9	
COSMO	a	30.1	55.6	24.7	71.2 <sup>a</sup>	10.8
	b		58.2	0	74.8	65.1
	c		80.4	23.6	100.1	10.8
	d		82.1 <sup>a</sup>	28.0	78.0 <sup>a</sup>	

<sup>a</sup> For these structures, frequency calculation yielded a second (low) negative eigenvalue; this could not be solved by further optimization and is attributed to the type of calculation rather than structural properties.

For the second step of the reaction, only the elimination of the apical group was investigated for the fluoride substituted system. In case of structure **5b**, this results in the elimination of HF instead of a condensation. In the case of the elimination of a water molecule, the most stable product complex (**6a**, Figure 11) was found to have an energy of 6.3 kJ/mol (10.8 kJ/mol) above that of **5b**, being close to isoenergetic to **5a** *in vacuo*. The product complex resulting from HF elimination (**6b**, Figure 11) is energetically far less favorable, having an energy of 54.6 kJ/mol (65.1 kJ/mol) relative to that of **5b** (Table 5). The energy of the transition state, however, is 59.9 kJ/mol relative to that of **5b**, thus considerably lower for the elimination of HF *in vacuo* than for the different condensation reactions (84.0, 77.3, and 105.9 kJ/mol for the elimination of water from **5a**, **5c**, and **5d**, respectively). With the COSMO model, the transition state energy for the elimination of HF (74.8 kJ/mol) is similar to those of the condensation reactions (71.2 kJ/mol for condensation from **5<sub>a</sub>** and 78.0 kJ/mol from **5<sub>d</sub>**); only the transition state for the condensation from **5<sub>c</sub>** lies significantly higher with 100.1 kJ/mol.

Geometric parameters of the fluoride substituted structures are in all cases very similar to those of the respective nonsubstituted structure. Si–F bonds were found to lie at 161–162 pm for tetracoordinated Si and range between 165 and 172 pm for the pentacoordinated silicon center in the intermediate. Details are listed in Supporting Information.



## Discussion

The calculations presented here reveal a reaction path for the condensation reaction of two molecules of silicic acid in a basic medium that proceeds through an intermediate structure, which contains a pentacoordinated silicon center. Different conformations of the intermediate represent the energetically most favorable stationary structure included in this study (energies of the presented systems are summarized in Table 4). The broad range of energies found for the intermediate is explained by the configuration of intramolecular hydrogen bonds. Those structures in which an apical and an equatorial hydroxido ligand on the pentacoordinated silicon center are aligned in a way that the apical hydroxyl group is not hydrogen bonded with its hydrogen atom toward an equatorial hydroxyl group were found to be unstable. In conformations where the apical hydroxyl group has a hydrogen bond to an equatorially bound oxygen atom, repulsions between the hydroxido ligands in a 90° angle around the Si(2) center are compensated by a hydrogen bond. These structures were calculated to be energetically more favorable than both the substrate and the product complex. Employment of the COSMO solvent model lowered the dependence of intermediate energy on the hydrogen bond configuration.

The observation of a reaction intermediate implies that models for the development of specific structures in silicates relying only on the thermodynamic product stability are not sufficient. In fact, the formation of the structure will also depend on the stabilization or destabilization of the corresponding intermediate and thereby on additional thermodynamic and kinetic parameters. The influence of structure-directing agents, as often used in zeolite synthesis, on the reaction path is subject to ongoing work in our group.

The different relative energies calculated for structure **2<sub>eq</sub>** and its transformation to **3** imply a lower activation barrier for the elimination from more highly substituted systems, as was found for the corresponding initial reactions of boron nitride formation.<sup>53,54</sup> This would explain the layered growth of silicates found by Agger et al.<sup>55</sup> as this mechanism is based on a higher condensation rate for more highly condensed silicon centers.

As calculations on structure **2<sub>eq</sub>** demonstrate, the stability of the intermediate is not necessarily transferable to more highly condensed systems. However, its high stability compared to a corresponding structure found in catalysis<sup>10</sup> under acidic conditions could be part of an explanation for the relative sensitivity of silicate systems toward basic hydrolysis. An attack of an anion OH<sup>-</sup> at the Si-center is facile.

The substitution of one hydroxido with a fluoro ligand was found to be a stabilizing effect on the intermediate structures in which it occupies the apical position or is bound to the silicon center that in turn is bound apically to the pentacoordinated silicon atom. For these isomers, the activation energy for the addition step is comparable to that found for the nonsubstituted system, while the addition toward an intermediate with equatorially bound fluoride is significantly hampered (though this might be due to the necessity of a simultaneous proton transfer). The elimination of a water molecule from the intermediate is thermodynamically more favored for the fluoride substituted system, though compared to the most stable intermediate it still is endergonic. The activation energy, however, is slightly higher. Only for the elimination of HF, the activation energy is considerably lower; the energy of the transition state is only 5.3 kJ/mol (9.7 kJ/mol) above that of the product, though here the product is clearly unfavorable.

In total, fluoride stabilizes the pentacoordinated intermediate structures relative to the monomer complexes and affects in addition the kinetics of formation of the silicate; HF is more easily eliminated from the system than water.

## Conclusions

In summary, we found that the condensation of two molecules of silicic acid is likely to proceed via a stable intermediate structure containing one pentacoordinated silicon center. The energies found for the transition states leading to this intermediate are reasonably low. The reaction barrier between the intermediate and the condensation product was found to be higher. However, it has to be remembered that the condensation step includes a proton transfer which, assuming water as the solvent, can proceed in a cascade over water molecules, lowering the energy of the transition state considerably. In our model presented, fluoride ions exert an influence on the thermodynamics of the reaction, stabilizing the dimeric structures, with the fluoride ion being easily exchangeable. Thus, we were able to present a viable model for the first steps of silicate condensation with and without fluoride catalysis.

**Acknowledgment.** The allocation of computing time by the Regionales Rechenzentrum of the University of Hamburg is gratefully acknowledged. M.H.P. thanks the DFG for a fellowship (PR 654/1-1). We thank Professor P. Behrens, University of Hannover, and Professor M. Fröba, University of Hamburg, for helpful discussions.

**Supporting Information Available:** Structures of transition states and Cartesian coordinates for all stationary structures (PDF). This material is available free of charge via the Internet at <http://pubs.acs.org>.

(53) Reinhardt, S.; Gastreich, M.; Marian, C. M. *Phys. Chem. Chem. Phys.* **2000**, *2*, 955–963.

(54) Reinhardt, S.; Gastreich, M.; Marian, C. M. *J. Phys. Chem. A* **2002**, *106*, 4205–4216.

(55) Agger, J. R.; Hanif, N.; Cundy, C. S.; Wade, A. P.; Dennison, S.; Rawlinson, P. A.; Anderson, M. W. *J. Am. Chem. Soc.* **2003**, *125*, 830–839.